

Analytical model for the effects of the variation of ferroelectric material parameters on the minimum subthreshold swing in negative capacitance capacitor

Raheela Rasool[†], Najeeb-ud-Din, and G. M. Rather

Department of Electronics and Communication, National Institute of Technology, Srinagar, Jammu & Kashmir, India

Abstract: In this paper, we analytically study the relationship between the coercive field, remnant polarization and the thickness of a ferroelectric material, required for the minimum subthreshold swing in a negative capacitance capacitor. The interdependence of the ferroelectric material properties shown in this study is defined by the capacitance matching conditions in the subthreshold region in an NC capacitor. In this paper, we propose an analytical model to find the optimal ferroelectric thickness and channel doping to achieve a minimum subthreshold swing, due to a particular ferroelectric material. Our results have been validated against the numerical and experimental results already available in the literature. Furthermore, we obtain the minimum possible subthreshold swing for different ferroelectric materials used in the gate stack of an NC-FET in the context of a manufacturable semiconductor technology. Our results are presented in the form of a table, which shows the calculated channel doping, ferroelectric thickness and minimum subthreshold for five different ferroelectric materials.

Key words: NC-capacitor; ferroelectrics; subthreshold swing; negative capacitance

Citation: R Rasool, Najeeb-ud-Din, and G M Rather, Analytical model for the effects of the variation of ferroelectric material parameters on the minimum subthreshold swing in negative capacitance capacitor[J]. *J. Semicond.*, 2019, 40(12), 122401. <http://doi.org/10.1088/1674-4926/40/12/122401>

1. Introduction

Negative capacitance field effect transistor (NC-FET) was proposed in 2008 by Salahuddin *et al.*^[1] to improve the subthreshold slope of the MOSFET. It has been experimentally proven by Asif *et al.* in Ref. [2]. Although many technologies^[3, 4] before it were suggested to improve the subthreshold slope of the MOSFET, they had inherent disadvantages that first had to be overcome. The NC-FET reduces subthreshold swing (SS) below Boltzmann's limit, due to the use of ferroelectric materials. The negative capacitance property of these materials, which actually reduces the SS, is entirely material and process dependent as described in phenomenological Landau-Devonshire theory^[5]. In an NC-FET, any ferroelectric material needs to be integrated directly within the gate stack of a conventional CMOS device and its properties determine the characteristics of the device. These materials are highly process and temperature dependent, and they can switch their properties from one state to another under certain conditions. The coercive field (E_C) and remnant polarization (P_0) of the material and process temperature determine the Landau parameters in Landau-Khalatnikov (LK)^[6, 7] equation described in the theory part of the paper.

In this paper, we have obtained an analytical equation to determine the thickness of the ferroelectric material required to get minimum subthreshold swing, under capacitance matching condition. The limit on minimum possible subthreshold swing (S_{\min}) reflects the choice of underlying MOS capacit-

ance (C_{MOS}) and ferroelectric capacitance (C_{FE}), which is fundamentally dictated by the need to stabilise the total NC capacitor capacitance. In section 2, we describe the fundamental capacitance constraints that define the minimum subthreshold swing in an NC capacitor. In section 3, we determine the optimal thickness of the ferroelectric material and substrate doping required to observe the NC effect for a minimum subthreshold swing. In section 4, we discussed the dependence of ferroelectric thickness on the coercive field and remnant polarization. Finally, in section 5 we obtain the equation for S_{\min} and corresponding S_{\min} for five different ferroelectric materials.

2. Fundamental considerations

For the analytical analysis of our model, we have considered a basic MOS capacitor with an extra ferroelectric layer in the gate stack. A schematic of a Metal-Ferroelectric-Metal-Insulator-Substrate (MFMIS) negative capacitance capacitor^[8] and its corresponding capacitance equivalent formed between the ferroelectric and the dielectric layer is shown in Figs. 1(a) and 1(b), respectively. The V_{GS} is the applied gate voltage and V_{GMOS} is the internal node voltage formed between the ferroelectric and the dielectric layer. Because our study examines the properties of a ferroelectric layer, we are not going to examine the electrical characteristics of the NC-FET and will instead limit our study to the capacitor only. The subthreshold swing (SS) of a MOSFET device is defined as the change in gate voltage (V_{GS}) required to change the drain current (I_D) by one order of magnitude^[9]. For the negative capacitance MOS capacitor equivalent shown in Fig. 1(b), SS is given as^[9]

Correspondence to: R Rasool, raheela_03phd14@nitsri.net

Received 13 FEBRUARY 2019; Revised 14 JUNE 2019.

©2019 Chinese Institute of Electronics

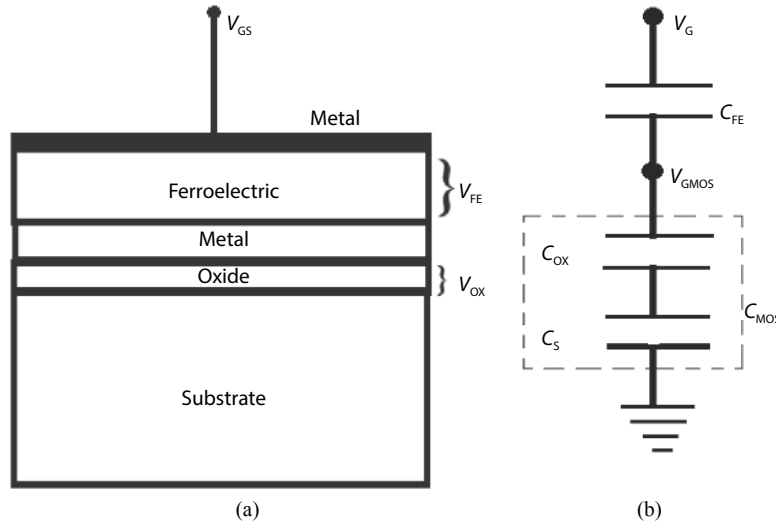


Fig. 1. (a) Schematic of MFMIS based NC-FET. (b) Equivalent capacitance divider.

$$SS \equiv \frac{\partial V_{GS}}{\partial (\log_{10} I_D)} = \frac{\partial V_{GS}}{\partial V_{GMOS}} \times \frac{\partial V_{GMOS}}{\partial (\log_{10} I_D)} = m \times n. \quad (1)$$

The SS can be reduced by reducing any of the two m or n factors. In the case of the NC capacitor, we are only concerned with the reduction of m to decrease the SS. The factor, $n = \frac{\partial V_{GMOS}}{\partial (\log_{10} I_D)} = \frac{2.3k_B T}{q}$ (k_B is Boltzmann's constant, T is temperature and q is electron charge) is known as transport factor and is ≈ 60 mV/decade at room temperature.

The unique property of NC effect in an MFMIS structure is to provide an internal voltage (V_{GMOS}) that is greater than the applied gate voltage (V_{GS}). From the capacitor divider formed in Fig. 1(b), the partial derivative of the V_{GS} with respect to V_{GMOS} , also known as body factor m , can be written as

$$m = \frac{\partial V_{GS}}{\partial V_{GMOS}} = 1 + \frac{C_{MOS}}{C_{FE}}, \quad (2)$$

where $\frac{1}{C_{MOS}} = \frac{1}{C_S} + \frac{1}{C_{OX}}$ is the series sum of substrate capacitance (C_S) and oxide capacitance (C_{OX}) capacitances.

To include the model for the dynamics of ferroelectric capacitor, the Landau Khalatnikov (LK) equation^[6, 7] that describes the correlation between the polarization and the electric field in a single domain ferroelectric material is employed. The voltage drop across the ferroelectric layer is given as

$$E = \frac{V_{FE}(Q)}{t_{FE}} = 2\alpha Q + 4\beta Q^3 + 6\gamma Q^5, \quad (3)$$

where α, β, γ are known as Landau parameters of the material. Furthermore, $\alpha < 0, \beta > 0, \gamma \geq 0$ defines the negative capacitance property, V_{FE} is the voltage drop across the ferroelectric film and t_{FE} is the thickness of the ferroelectric layer. The total charge Q is the same as the total charge in the channel, which is calculated using the depletion width approximation and has already explained in Ref. [10]. The potential balance in the equivalent capacitor network results in applied gate voltage V_{GS} as the sum of the voltage drop across the ferroelectric capacitor (V_{FE}) and the internal node voltage V_{GMOS} is given as

en as

$$V_{GS} = V_{FE} + V_{GMOS}, \quad (4)$$

where $V_{GMOS} = V_{OX} + \psi_S + V_{FB}$ and where V_{FB} is the flat-band voltage, V_{OX} is the voltage across the oxide layer between ferroelectric and silicon substrate and ψ_S is the surface potential or band bending in the semiconductor. The capacitance C_{FE} is the differential capacitance of ferroelectric layer and is defined dQ/dV_{FE} . From the LK equation described in Eq. (3), the inverse of C_{FE} is obtained as

$$C_{FE}^{-1}(Q) = (2\alpha + 12\beta Q^2 + 30\gamma Q^4) t_{FE}. \quad (5)$$

The total gate capacitance C_T of the NC capacitor is given by

$$C_T^{-1}(Q) = C_{MOS}^{-1}(Q) + C_{FE}^{-1}(Q). \quad (6)$$

The increased gate capacitance due to C_{FE} of the ferroelectric layer in the gate stack, amplifies the internal node voltage. However, C_T must be positive for all charges for a hysteresis free stable operation of the device^[11-13]. This stability requirement puts a fundamental constraint on C_{MOS} ; i.e.,

$$C_{MOS}(Q)^{-1} \geq |C_{FE}^{-1}(Q)|, \quad (7)$$

which should hold throughout the NC regime. Eq. (7) puts a minimum limit on the subthreshold swing that can be obtained in an NC-FET. For a given dependence of C_{MOS} and C_{FE} on Q , minimum SS can be obtained where the two capacitances match as closely as possible^[12, 14]. However, the two cannot be made equal because they have different dependence on the value of Q and it is not possible to obtain the same values for all of the values of Q .

For a fixed C_{OX} , C_{MOS} changes with C_S which depend on the channel doping N_A ; however, C_S depends on whether the channel is in subthreshold, where $C_S(Q) \propto \frac{N_A}{Q}$, or in inversion, where $C_S(Q) \propto Q$.

Unlike conventional MOSFETs, where the minimum value of SS is fixed at 60 mV/dec, there is no such single value in NC-FET. The minimum subthreshold swing (S_{min}) that character-

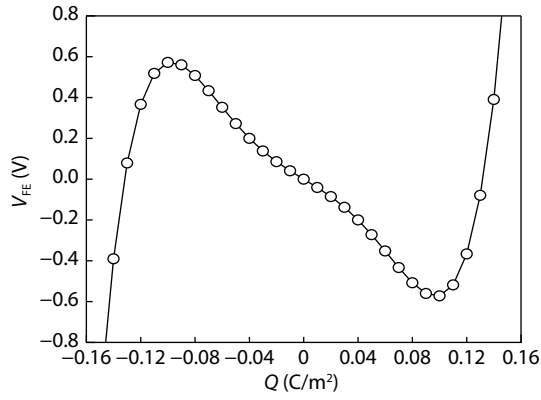


Fig. 2. Voltage-charge plot for a ferroelectric material.

izes the NC-FET is different for different devices. However, the two necessary conditions for minimum subthreshold swing are a) $C_{\text{MOS}}(Q) \leq -C_{\text{FE}}(Q)$ and b) channel should be in subthreshold throughout the NC regime^[15] remain the same.

Mathematically, the condition for being in subthreshold is given by $\psi_s < 2\psi_B = \frac{2k_B T}{q} \ln\left(\frac{N_A}{n_i}\right)$ (where ψ_s is the surface potential, ψ_B is the built-in potential on p-substrate, N_A is the substrate doping and n_i is the intrinsic carrier concentration), throughout the NC-regime. For uniform substrate doping and the partially depleted case, ψ_s is related to the depletion charge Q by^[9]

$$\psi_s = \frac{Q^2}{2q\epsilon_0\epsilon_s N_A}, \quad (8)$$

where ϵ_0 is the permittivity of free space and ϵ_s is the permittivity of silicon substrate. The condition for subthreshold region translates Eq. (8) into $l/\psi_B = \frac{Q^2}{2q\epsilon_0\epsilon_s N_A}$, where $l < 2$.

Condition (7) is general and will work irrespective of values of C_{MOS} and $|C_{\text{FE}}|$. However, Eq. (8) changes as we change the FET structure, such as single gate versus multigate^[16] or bulk FET versus depleted FET.

3. Optimal ferroelectric thickness

Fig. 2 shows the $V_{\text{FE}}-Q$ characteristics of the ferroelectric material. V_{FE} decreases in the range of $-Q_1 < Q < +Q_1$ and hence C_{FE} is also negative between $-Q_1$ and $+Q_1$. However, an n-channel NC-FET must be operated in the $Q > 0$ branch of the NC regime, so that it can be balanced by the negative charges of the channel. Therefore, $Q_2 = 0$ is defined as the other boundary of the negative capacitance regime. At $Q_2 = 0$, Eq. (4) reduces to $C_{\text{FE}}(Q) = \frac{1}{2\alpha t_{\text{FE}}}$ and at flatband capacitance of the underlying MOS capacitance is given by^[17]

$$\frac{1}{C_{\text{MOS}}} = \sqrt{\frac{v_t}{q\epsilon_0\epsilon_s N_A}} + \frac{1}{C_{\text{OX}}}, \quad (9)$$

where $v_t = K_B T/q$ is the thermal voltage. Therefore, the condition in Eq. (7) for minimum subthreshold swing and hysteresis free operation of the device can be translated into

$$t_{\text{FE}} = -\frac{1}{2\alpha} \left[\frac{1}{C_{\text{OX}}} + \sqrt{\frac{v_t}{q\epsilon_0\epsilon_s N_A}} \right], \quad (10)$$

which relates t_{FE} , α and N_A for minimum subthreshold slope.

In addition, Q_1 is the maximum charge value and Eq. (8) becomes

$$N_A = \frac{Q_1^2}{2q\epsilon_0\epsilon_s l\psi_B}. \quad (11)$$

The final equation for the optimized ferroelectric thickness is

$$t_{\text{FE}} = -\frac{1}{2\alpha} \left[\frac{1}{C_{\text{OX}}} + \sqrt{\frac{2v_t 2\psi_B}{Q_1^2}} \right]. \quad (12)$$

Thus, for a given ferroelectric material characterized by α , β , and γ , SS is minimized for N_A and t_{FE} given by Eqs. (11) and (12). It is clear from this equation that the thickness of ferroelectric material required depends on the Landau parameter α of the material and the capacitance of the oxide between the ferroelectric and the silicon substrate. It is evident that high value of parameter α reduces the optimal ferroelectric thickness for a minimum subthreshold swing.

4. Dependence on coercive field (E_C) and remnant polarization (P_0)

The anisotropy constants α and β in Landau equation are calculated by fitting the $Q-V_{\text{FE}}$ characteristics to yield the given value of coercive field E_C and the remnant polarization P_0 . Hence, $V_{\text{FE}}(Q = P_0) = 0$ and $dV_{\text{FE}}/dQ(V_{\text{FE}} = E_C t_{\text{FE}}) = 0$. Consequently, the equation for α and β becomes

$$\alpha = \frac{3\sqrt{3} E_C}{4 P_0}, \quad \beta = \frac{3\sqrt{3} E_C}{8 P_0^3}. \quad (13)$$

Therefore, the thickness of the ferroelectric film in terms of coercive field and remnant polarization can be obtained as

$$t_{\text{FE}} = \frac{2 P_0}{3\sqrt{3} E_C} \left(\frac{1}{C_{\text{OX}}} + \sqrt{\frac{2v_t 2\psi_B}{Q_1^2}} \right), \quad (14)$$

the high coercive field and small remnant polarization results in small t_{FE} .

Ignoring the higher terms of Q in the Eq. (5), the ferroelectric negative capacitance equation reduces to

$$C_{\text{FE}} = \frac{1}{2\alpha t_{\text{FE}}} = -\frac{2 P_0}{3\sqrt{3} E_C t_{\text{FE}}}. \quad (15)$$

In an NCFET device, the improved $I_{\text{ON}}/I_{\text{OFF}}$ ratio and small subthreshold swing without hysteresis in the transfer characteristics depends on the capacitance matching ($|C_{\text{FE}}| > C_{\text{MOS}}$) or $|C_{\text{FE}}| \approx C_{\text{MOS}}$ as already discussed^[12, 13]. For the best results, $|C_{\text{FE}}|$ should be as close as possible to C_{MOS} , or should be higher than the C_{MOS} . Based on the values of N_A and t_{FE} obtained for the material PZT, C_{MOS} and $|C_{\text{FE}}|$ shown in Fig. 3(a), suggesting $|C_{\text{FE}}(Q)| \geq C_{\text{MOS}}(Q)$ at each Q , as in the numerical simulation for the same material in the MFIS capacitor^[18]. The corresponding V_{FE} and V_{GMOS} obtained from numerical simulations of MFIS capacitor are shown in Fig. 3(b). It is clear that with the increase in Q , V_{FE} decreases and this in turn amplifies V_{GMOS} , and reduces SS below Boltzmann's limit of 60 mV/dec.

The higher values of C_{FE} due to smaller α is due to small E_C and large P_0 for fixed ferroelectric thickness, which res-

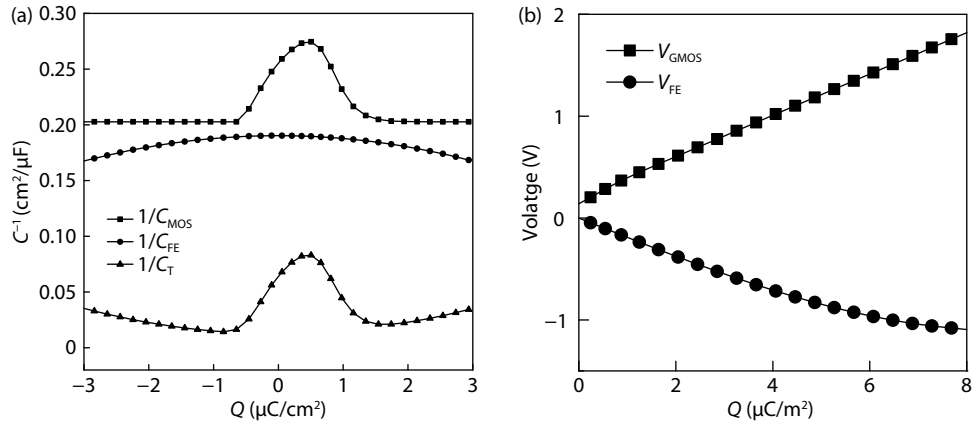


Fig. 3. (a) Capacitance versus charge plots for MOS capacitor, ferroelectric capacitor and the total capacitance of MFMS capacitor. (b) Voltage charge plot of the MFMS capacitor.

Table 1. Ferroelectric thickness (t_{FE}) and minimum subthreshold swing (S_{min}) for different ferroelectric materials.

Parameter	PZT ^[20]	BaTiO ₃ ^[15]	SBT ^[15]	HfSiO ₂ ^[22]	P(VDF-TrFE) ^[23]
α (cm/F)	-2.25×10^9	-5×10^8	-3.25×10^9	-8.65×10^{10}	-1.8×10^{11}
β ($\text{cm}^3/\text{F}/\text{C}^2$)	1.3×10^{18}	2.2×10^{18}	9.37×10^{18}	1.92×10^{20}	5.8×10^{22}
γ ($\text{cm}^5/\text{F}/\text{C}^4$)	9.83×10^{25}	7.5×10^{27}	0	0	0
N_{A} (cm^{-3})	2.3×10^{20}	3.3×10^{20}	7.5×10^{19}	5.7×10^{19}	4×10^{18}
t_{ox} (nm)	2	2	2	2	2
t_{FE} (nm)	22.3	19.3	15.5	5.8	2.8
S_{min} (mV/dec)	52.8	46.5	41.6	31	27

ults in lower voltage step up $\left(\frac{\partial V_{\text{MOS}}}{\partial V_{\text{GS}}} = \frac{C_{\text{FE}}}{C_{\text{FE}} - C_{\text{MOS}}}\right)$. Therefore, the gain reduces and consequently I_{ON} decreases. Although an increase in P_0 reduces the hysteresis due to positive total gate capacitance, it comes at the cost of reduction in $I_{\text{ON}}/I_{\text{OFF}}$ which renders ineffective the primary advantage of using ferroelectric in gate stack^[19].

Similarly, high values of α implies a proportionally low value of $|C_{\text{FE}}|$ for a fixed t_{FE} . This can also be understood in terms of very high coercive field and low remnant polarization. The higher values of α results in the smaller $|C_{\text{FE}}|$ than C_{MOS} , results in total negative capacitance which appears as the hysteresis in the transfer characteristics of the devices^[20]. Therefore, a high coercive field improves the $I_{\text{ON}}/I_{\text{OFF}}$ ratio; however, hysteresis occurs in the characteristics due to instability.

Consequently, we come to the conclusion that in an NC capacitor using ferroelectric material, the material parameters and the thickness of the material are interdependent to achieving a good result.

Considering Eq. (14), a high P_0 and low E_{C} results in higher t_{FE} ; whereas, a low P_0 and high E_{C} results in smaller t_{FE} . The calculated values of t_{FE} can be used to stabilise the capacitance and enhance the capacitance matching to the obtain the best possible results with high I_{ON} and no hysteresis. Therefore, we can opt for either higher polarization and smaller E_{C} or higher E_{C} with smaller P_0 . However, from the design perspective of the NC-FET as experimentally shown in Ref. [20], the gate stack with ferroelectric material giving high E_{C} and low P_0 resulted in 45% higher I_{ON} with the same OFF current. Therefore, we can say that higher alpha and consequently lower t_{FE} results in better characteristics and are also viable from the point of view of scaling these devices.

5. Equation for minimum subthreshold swing

Unlike $S_{\text{min}} = 60$ mV/dec for classical FETs, a single S_{min} does not define the performance of all NCFETs; instead the stability constrained S_{min} depends on the choice of material system and channel type. In this section, an explicit analytical equation has been obtained to calculate the minimum possible SS (S_{min}) under capacitance matching conditions. From the calculated S_{min} for different materials, we can infer the viability of different materials for the designing of NC-FETs.

For a given ferroelectric material characterised by α , β and γ subthreshold swing is minimized for N_{A} and t_{FE} given in Eqs. (11) and (12). The equation for minimum subthreshold swing (S_{min}) is obtained by substituting the value of C_{FE} in Eq. (2) and can be written as

$$S_{\text{min}} \approx \frac{2.3k_{\text{B}}T}{q} (1 + M \times t_{\text{FE}}), \quad (16)$$

where $M = (2\alpha + 12\beta Q^2 + 30\gamma Q^4) C_{\text{MOS}}$ is a material dependent constant. The values of calculated optimal thicknesses and corresponding S_{min} for the five different ferroelectric materials viz: lead zirconium titanate (PZT), strontium barium titanate (SBT), barium titanate (BaTiO₃), hafnium silicate (HfSiO) and organic ferroelectric material P(VDF-TrFE) are given in Table 1. The non-ideal effects (such as domain propagation, grain boundaries and domain nucleation of the ferroelectric material) degrade the subthreshold swing of the realistic device and, therefore, the minimum subthreshold swing (S_{min}) in Eq. (16) can be obtained when we assume that the all these non-idealities are absent^[21]. The value of S_{min} for PZT material is 52.8 mV/dec using the above equation, which is consistent with the simulated value of 55 mV/dec for the

same material by Ref. [23]. Furthermore, the value of 27 mV/dec for the organic ferroelectric material PVDF is in agreement with low SS values for such materials, as described in Ref. [24].

6. Conclusion

In this paper, we have developed an analytical equation for the ferroelectric thickness and the minimum subthreshold swing possible in an MFMS capacitor. This captures the impact of ferroelectric material properties on the Landau coefficients, which in turn determines the thickness of the ferroelectric material required to have better capacitance matching and which reduces the subthreshold swing. Finally, this study calculated the minimum subthreshold swing of an NC capacitor with five different ferroelectric materials, which may help us in the selection of a particular ferroelectric material for an actual NC-FET design.

References

- [1] Salahuddin S, Datta S. Use of Negative capacitance to provide voltage amplification for low power nanoscale devices. *Nano Lett*, 2008, 8(2), 405
- [2] Khan A I, Bhowmik D, Yu P, et al. Experimental evidence of ferroelectric Negative capacitance in nanoscale heterostructures. *Appl Phys Lett*, 2011, 99(11), 113501
- [3] Seabaugh A C, Zhang Q. Low-voltage tunnel transistors for beyond CMOS logic. *Proc IEEE*, 2010, 98(12), 2095
- [4] Gopalakrishnan K, Woo R, Jungemann C, et al. Impact ionization MOS (I-MOS) -Part I: Device and circuit simulation. *IEEE Trans Electron Devices*, 2005, 52(1), 69
- [5] Devonshire A F. Theory of ferroelectrics. *Adv Phys*, 1954, 3(10), 85
- [6] Rabe K M, Ahn C H, Triscone J M. Physics of ferroelectrics: a modern perspective. Berlin: Springer, 2007
- [7] Ginzburg V L. Phase transitions in ferroelectrics: some historical remarks. *UFN*, 2001, 171(10), 1091
- [8] Rusu A, Salvatore G A, Jimenez D, et al. Metal-ferroelectric-metal-oxide semiconductor field effect transistor with sub-60mV/decade subthreshold swing and voltage amplification. *IEEE International Electron Devices Meeting*, 2010, 6.3.1
- [9] Taur Y, Ning T. Fundamentals of Modern VLSI device. Cambridge: Cambridge University Press, 1998.
- [10] Rasool R, Rather G M, ud-Din N. Analytic model for the electrical properties of negative capacitance metal-ferroelectric-insulator-silicon (MFIS) capacitor. *Integrated Ferroelectrics*, 2017, 185, 93
- [11] Jain A, Alam M A. Prospects of hysteresis free abrupt switching (0 mV/decade) in Landau switches. *IEEE Trans Electron Devices*, 2013, 60(12), 4269
- [12] Khan A I, Yeung C W, Hu C, et al. Ferroelectric negative capacitance MOSFET: Capacitance tuning & antiferroelectric operation. *IEDM Tech Dig*, 2011, 255
- [13] Seeger J I, Crary S B. Analysis and simulation of MOS capacitor feedback for stabilizing electrostatically actuated mechanical devices. *Trans Built Environ*, 1997, 31(13), 1
- [14] Krowne C W, Kirchoefer S W, Chang W, et al. Examination of possibility of negative capacitance using ferroelectric materials in solid state electronic devices. *Nanoletters*, 2011, 11(3), 988
- [15] Jain A, Alam M A. Stability constraints define the minimum subthreshold swing of a negative capacitance field-effect transistor. *IEEE Trans Electron Devices*, 2014, 61(7), 2235
- [16] Jiménez D, Miranda E, Godoy A. Analytic model for the surface potential and drain current in negative capacitance field-effect transistors. *IEEE Trans Electron Devices*, 2010, 57(10), 2405
- [17] Pierret R F. Semiconductor device fundamentals. Pearson, 1995
- [18] Dasgupta S, Rajashekhar A, Majumdar K, et al. Sub-KT/Q switching in strong inversion in $\text{PbZr}_{0.52}\text{Ti}_{0.4}\text{O}_3$ gated negative capacitance FETs. *IEEE J Explor Solid State Comput Devices Circuits*, 2015, 1, 43
- [19] Lee H, Yoon Y, Shin C. Current voltage model for negative capacitance field effect transistors. *IEEE Electron Device Lett*, 2017, 38(5), 669
- [20] Lin C I, Khan A I, Salahuddin S, et al. Effects of the variation of ferroelectric properties on negative capacitance FET characteristics. *IEEE Trans Electron Devices*, 2016, 63(5), 2197
- [21] Cano A, Jimenez D. Multidomain ferroelectricity as a limiting factor for voltage amplification in ferroelectric field-effect transistors. *Appl Phys Lett*, 2010, 97(13), 133509
- [22] Boscke T S, Muller J, Bruhaus D, et al. Ferroelectricity in hafnium oxide: CMOS compatible ferroelectric field effect transistors. *IEE Electron Devices Meeting*, 2011, 24
- [23] Li Y, Lian Y, K Yao K, et al. Evaluation and optimization of short channel ferroelectric MOSFET for low power circuit application with BSIM₄ and Landau theory. *Solid State Electron*, 2015, 114, 17
- [24] Saeidi A, Jazaeri F, Stolichnov I, et al. Double-gate negative-capacitance MOSFET with PZT gate stack on ultra thin body SOI: An experimentally calibrated simulation study of device performance. *IEEE Trans Electron Devices*, 2016, 63(12), 4678